

## Aerodynamic Analyses of Aircraft-Blended Winglet Performance

Hesham S. M. Helal<sup>1</sup>, Essam E. Khalil<sup>2</sup>, Osama E. Abdellatif<sup>3</sup>, Gamal M. Elhariry<sup>4</sup>

<sup>1</sup>PhD student, Airworthiness Inspector at Egyptian Aviation Authority, Egypt.

<sup>2</sup>Professor of Mechanical Power Engineering, Cairo University, Egypt, Fellow AIAA.

<sup>3</sup>Professor of Mechanical Power Engineering, Benha University, Egypt.

<sup>4</sup>Assistant Professor of Mechanical Power Engineering, Cairo University, Egypt.

---

**Abstract:** Winglets have become popular additions to high speed aircraft wanting to increase fuel efficiency by reducing drag from wingtip vortices. Numerical studies have been carried out to investigate the best aerodynamic performance of a subsonic aircraft wing at various cant angles of winglets. This analytical study includes NACA653218 airfoil section coordinates for the wing design and the winglet with the blended design. In this Paper, a numerical validation procedure by FLUENT®6.3.26, computational fluid dynamics software with The Spalart-Allmaras turbulence model is described for determination and estimation aerodynamic characteristics for three dimensional subsonic rectangular wing (with NACA65-218 airfoil section). It is observed that in the present work there is a fair agreement between the numerical and the experimental studies. This Paper studies blended winglet with different angles at (30, 45, 60, and 90) on the wing. The wing is drawn using Gambit 2.4.6 with a chord length of 1.755 m. The NACA 65-218 airfoil is extruding by 14.7 m with wing taper ratio equal to 0.4. The winglets are created with the same airfoil at the tip wing with taper ratio equal to 0.5. The winglet length is about 17 % of the semi-span of the wing. The connection between the wing and the winglet is a curved edge. From CFD models run at a Mach number of 0.2 at sea level, the pressure and temperature of air at this height are 101325 pa and 288.2 K, respectively, and the results show that the wing with winglet can increase lift to drag (L/D) ratio by approximately 6% to 15% more than wing without winglet. It depends on angle of attack along the different phases of flight, and show the most efficient angle of attack occurs at 4 degrees.

**Keywords:** Blended, winglet, Induce drag, Lift, Vortices, Aircraft.

---

### I. Introduction

A winglet is a device used to improve the efficiency of aircraft by lowering the lift induced drag caused by wingtip vortices [1]. It is a vertical or angled extension at the tips of each wing. Winglets improve efficiency by diffusing the shed wingtip vortex, which in turn reduces the drag due to lift and improves the wing's lift over drag ratio. Winglets increase the effective aspect ratio of a wing without adding greatly to the structural stress and hence necessary weight of its structure. Research into winglet technology for commercial aviation was pioneered by Richard Whitcomb in the mid 1970's. Small and nearly vertical fins were installed on a KC-135A and flights were tested in 1979 and 1980 [2] & [3]. Whitcomb, [2] & [3] revealed that in full size aircraft, winglets can provide improvements in efficiency of more than 7%. For airlines, this translates into millions of dollars in fuel costs. Winglets are being incorporated into most new transport aircraft, including business jets, the Boeing 747-400, airliners, and military transport. The wingtip sail was the first industry application winglet studied by the Pennsylvania State University (PSU) [4].

In general any wingtips that do not end the wing simply horizontally are considered as some kind of a winglet.

Basically five types of winglets exist,

- Blended Winglets
- Wingtip Fences
- Raked Wingtips
- Spiroid Winglet
- Wing-grid as wing tip

#### 1.1 BLENDED WINGLETS (The Real Winglets):

A blended winglet as shown in Figure 1 is attached to the wing with smooth curve instead of a sharp angle and is intended to reduce interference drag at the wing/winglet junction. A sharp interior angle in this region can interact with the boundary layer flow causing a drag inducing vortex, negating some of the benefit of the winglet. The blended winglet is used on business jets and sailplanes, where individual buyer preference is an important marketing aspect



**Figure1:** Blended Winglet Examples [5].

### 1.2 Wingtip Fences:

These are a special variant of winglets that extend both upward and downward from the tip of the wing as shown in Figure2. Preferred by European plane-maker Airbus, it is featured on their full product range (except the A330/340 family and the future A350).



**Figure2:** Wingtip Fence A380[6].

### 1.3 Raked Wingtips:

The raked tip is attached with the main wingtip with higher angle of sweep than the main wing. Boeing 777 long-range jets have been designed with raked wingtip, as shown in Figure3.



**Figure3:** Raked Wingtips on Boeing 777 Long-Range Jets [7]

### 1.4 Spiroid Winglet

One end of the spiroid tip is attached to the forward part of the wing tip and continues to form a spiral loop which ends at the aft portion of the wing tip, as shown in Figure4. Hence it looks oval shaped when viewed from front. Spiroid tipped wing was created to reduce the induced drag and also to reduce the noise effects associated with the tip vortices.



**Figure4:** Spiroid Tipped Wing [8]

### 1.5 Wing-grid as wing tip

Wing grid geometry is defined by two or more wing like surfaces running parallel to each other from the end of wing section which forms the grid, as shown in Figure5.



**Figure5:**Wing Grids as Wing End Section [9]

## II. Governing Equations

The air flow is modelled as 3-D compressible viscous flow. Thus the governing equations are the continuity equation together with x- y and z- Navier-Stokes equations for a compressible flow. Turbulence is modelled by the Spalart-Allmaras model. The complete system of equations is presented here in differential form, FLUENT® Documentation [10] and [11]. The governing equations in this model are:

### 2.1. Continuity equation in vector form:

$$\frac{\partial \rho}{\partial t} + \nabla \cdot (\rho \vec{V}) = 0$$

### 2.2. Momentum equation in vector form:

$$\nabla \cdot (\rho \cdot \vec{v} \vec{v}) = -\nabla p + \nabla \cdot (\bar{\tau}) + \vec{F}$$

### 2.3. Energy Conservation Equation:

$$\frac{\partial(\rho E)}{\partial t} + \nabla \cdot (\vec{v} (\rho E + p)) = \nabla \cdot \left[ k_{eff} \nabla T - \sum_j h_j \vec{J}_j + (\bar{\tau}_{eff} \cdot \vec{v}) \right] + S_h$$

## III. Validation Procedures

A similar Numerical Model Rectangular wing with winglet at a Cant angle 0° is illustrated in Figure6. Wing and winglet cross sections are NACA65<sub>3</sub>218 airfoil section. A similar Numerical Model of the same previously-mentioned grid size and type was developed, for verifying the numerical model with the literature experiment and numerical model. Measurements were used to verify the work made by [12]. The tests are performed on a rectangular wing a chord length of 121mm and a semi-span of 330mm and winglet dimension is a Cant angle 0°, the winglet a Tip chord of 60.5 mm and a length of 55.1 mm.

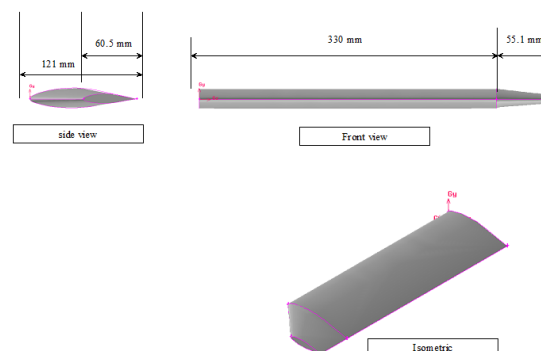


**Figure 6:** Rectangular Wing With Winglet at Cant Angle 0° And NACA653218 Airfoil Section

The boundary condition is the same as in rectangular wing. The Reynolds number ( $Re=2.89 \times 10^5$ ) as shown in Figure 7, from literature review, experimental data from [12], in order to validate the present simulation. The free stream temperature is 288.2 K, which is the same as the environmental temperature. The density of the air at the given temperature is  $\rho=1.225 \text{ kg/m}^3$ , the pressure is 101325 Pa and the viscosity is  $\mu=1.7894 \times 10^{-5} \text{ kg/m s}$ . A segregated, implicit solver is utilized (ANSYS FLUENT® processor) Calculations are done for angles of attack ranging from  $0^\circ$  to  $12^\circ$ . The wing profile, boundary conditions and meshes are all created in GAMBIT® 2.3.16 as a pre-processor.

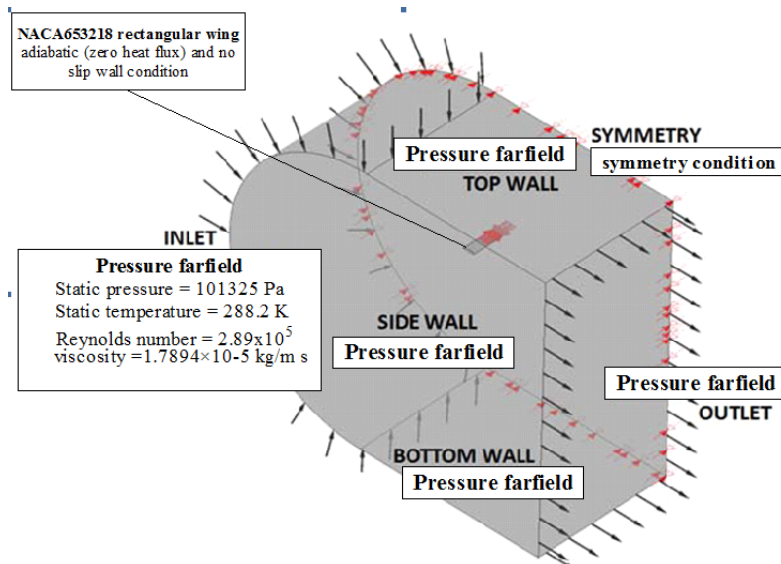


**Figure 7:** Numerical Model of NACA653218 Rectangular Wing [12].

The volume must be dense enough and computed fields must be large enough to satisfy far field boundary conditions. 3D unstructured tetrahedral mesh is used for complex shape of winglet, as shown in Figure 8.

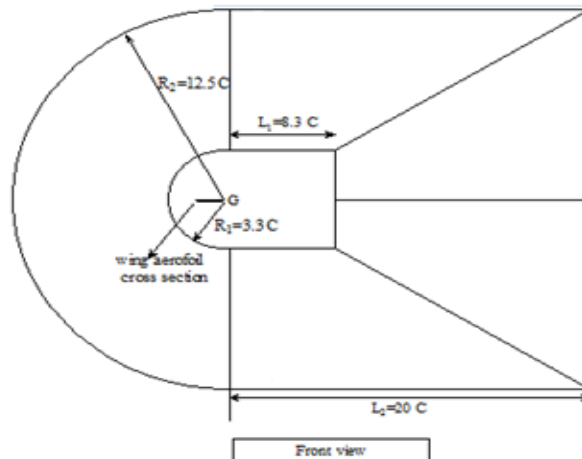


**Figure 8:** Front View Computed Flow Field for Rectangular Wing With NACA653218 Airfoil Section.

### 3.2 Grid dependency check

The first step in performing a CFD simulation should be to investigate the effect of the mesh size on the solution results. Generally, a numerical solution becomes more accurate as more cells are used, but using additional cells also increases the required computer memory and computational time. To examine the independency of the results to cell number, five different mesh sizes were generated. The results of these five meshes are shown in table 1, Lift coefficient at different number of grid cells for an angle of attack ( $0^\circ$ ) are indicated.

**Table1:** Comparison of Five Kinds of Meshing With Different Number of Cells

Cell number	434441	855160	1462861	2173368	4703836
$C_L$	0.1079	0.1084	0.1085	0.1087	0.1088

In order to save time when running the computations, the grid with the smallest number of cells displaying an independent solution should be used for the calculations. This is seen to be the case for a grid with around 2250000 cells. The Rectangular wing with NACA65<sub>3</sub>218 airfoil section model was used to verify the work done by [12] and [13]. Compare the results of the numerical model by Spalart-Allmaras model to those of the experimental and numerical models measurements. The results show good agreement of lift coefficient with the corresponding values in the experimental and numerical models measurements as shown as Figure 9.

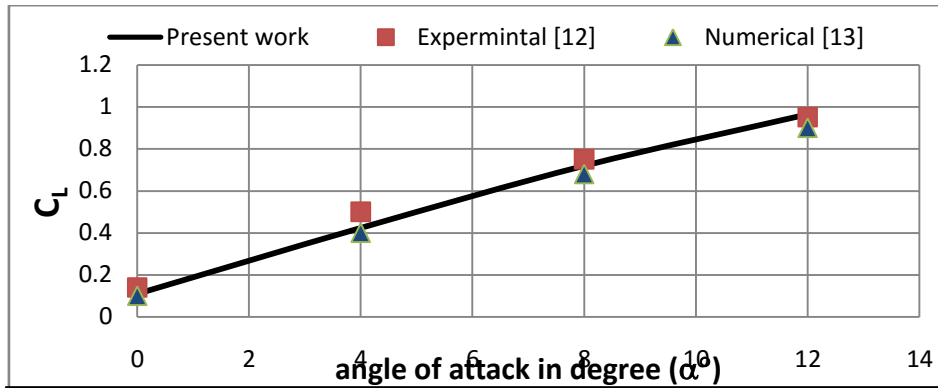


**Figure 9:** Numerical results of CL in Comparison to Corresponding Experimental and Numerical Results

#### IV. Effect Ofblended Wingleton Aircraft Wing

This paper shows the difference between wing without winglet and with Blended winglet. According to an airfoil database, scatter diagram of an airfoil used is a 5-digit NACA series, NACA 65-218 airfoil. The airfoil is drawn using Gambit with a chord length at root 4.17 m and tip 1.755 m. The NACA 65-218 airfoil is extruding by 14.7 m with a taper ratio of 0.4 and, incidence angle at root 3 degree and incidence angle at tip 0 degree, the Blended winglet is drawn with four angles ( $\theta = 30, 45, 60$  and  $90$  degree), for four cases study. The winglet length is about 17 % of the semi-span of the wing. The connection between the wing and the winglet is a curved edge as shown in Figure 10. The wing will run at a Mach number of 0.2 at the sea level. The pressure and the temperature of air at sea level are 101325 pa and 288.2 K, respectively.

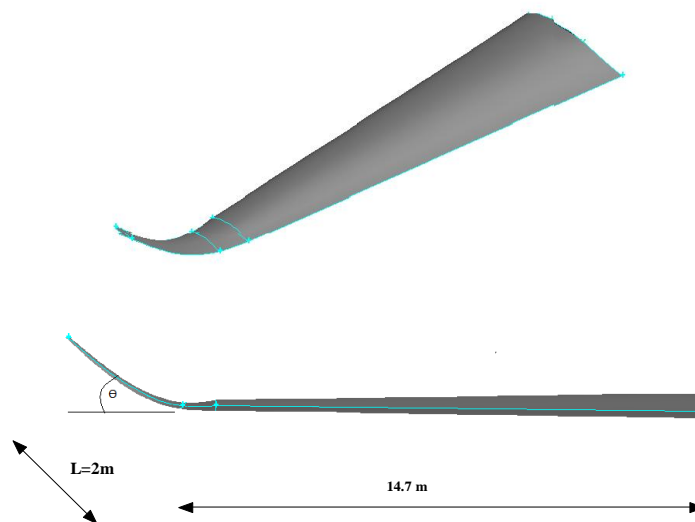


**Figure 10:** Wing with Blended Winglets with NACA 65-218 Airfoil Section.

#### V. Results And Discussion

From CFD model we determine lift, drag, pressure contours and pathlines around wing at all AOA.

**5.1 Lift Coefficient (CL), Drag Coefficient (CD) and Lift-To-Drag Ratio (CL/CD) Analysis**

The coefficient of lift versus angle of attack for the aircraft wing with and without winglet studied investigation as shown in Figures 11, 12 and 13 at Mach number equal to 0.2. The figures show that the CL increases with increase in angle of attack. Table 2, 3 and 4 show the wing with blended winglet and without winglet the value of lift, drag and lift-to-drag ratio coefficient. The Lift-To-Drag Ratio (CL/CD) is increasing about 3 to 15% along angle of attack more than wing without winglet and reaches max at angle of attack of 4 degree, as shown in Figure 13.

**Table 2:** Lift coefficient (CL) Comparison between Wing without Winglet and with Blended Winglet Configurations

Winglet configuration	$\alpha=0^\circ$	$\alpha=4^\circ$	$\alpha=8^\circ$	$\alpha=12^\circ$	
Wing without winglet	0.31519	0.6535	0.94945	1.16415	
Wing with Blended winglet	$\theta=30$	0.34130	0.74677	1.09709	1.34215
	$\theta=45$	0.33887	0.72725	1.02653	1.31411
	$\theta=60$	0.33617	0.71427	1.04252	1.27416
	$\theta=90$	0.33422	0.74343	1.02214	1.24873

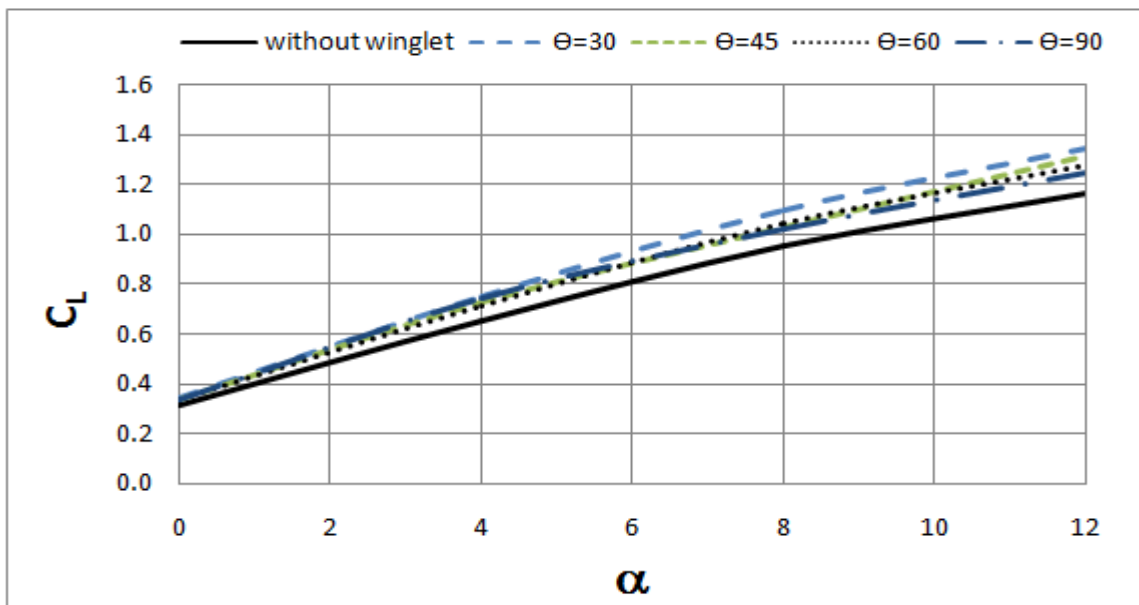


**Figure 11:** Lift coefficient (CL) Comparison between Wing without Winglet and with Blended Winglet Configurations, Versus Angle of Attack ( $\alpha$ ).

**Table 3:** Drag coefficient (CD) Comparison between Wing without Winglet and with Blended Winglet Configurations

Winglet configuration	$\alpha=0^\circ$	$\alpha=4^\circ$	$\alpha=8^\circ$	$\alpha=12^\circ$	
Wing without winglet	0.04770	0.07539	0.12755	0.20185	
Wing with Blended winglet	$\theta=30$	0.05040	0.07804	0.13249	0.21205
	$\theta=45$	0.04939	0.07674	0.12959	0.21305
	$\theta=60$	0.04855	0.07565	0.12747	0.20242
	$\theta=90$	0.04813	0.07355	0.12607	0.19957



**Figure12:** Drag coefficient (CD) Comparison between Wing without Winglet and with Blended Winglet Configurations, Versus Angle of Attack ( $\alpha$ ).

**Table4:** Lift-To-Drag Ratio (CL/CD) Comparison between Wing without Winglet and with Blended Winglet Configurations

Winglet configuration		$\alpha=0^\circ$	$\alpha=4^\circ$	$\alpha=8^\circ$	$\alpha=12^\circ$
Wing without winglet		6.60776	8.66858	7.44376	5.76754
Wing with Blended winglet	$\theta=30$	6.77255	9.56923	8.28074	6.32928
	$\theta=45$	6.86099	9.47673	7.92126	6.16807
	$\theta=60$	6.92458	9.44124	8.17879	6.29458
	$\theta=90$	6.94390	10.10768	8.10804	6.25721

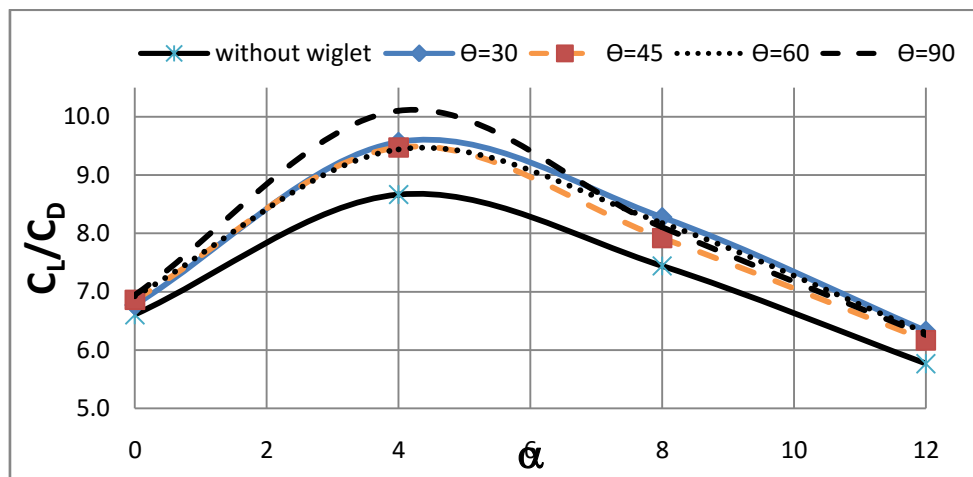


**Figure13:** Lift-To-Drag Ratio (CL/CD) Comparison between Wing without Winglet and With Blended Winglet Configurations, Versus Angle Of Attack ( $\alpha$ ).

## VI. Conclusions

From the CFD solution, the figures show that how wingtip vortices occur and it will increase with increasing angle of attack and the wing with winglet decrease wingtip vortices at high angle of attack. We examined the Blended winglet for different angles at ( $\Theta=30^\circ$ ,  $45^\circ$ ,  $60^\circ$  and  $90^\circ$ ). The winglets improved lift to drag ratio (L/D) by increasing about 3% to 15% compared with wing without winglet. The optimum angle was at  $\theta=90^\circ$  at angle of attack equal  $4^\circ$ . Finally, the wing with winglet is better than wing without winglet and increase (L/D) ratio.

## References

- [1] Yates, J. E., and Donaldson, C., "Fundamental Study of Drag and an Assessment of Conventional Drag-Due-To-Lift Reduction Devices", NASA Contract Rep 4004, 1986
- [2] Whitcomb, R. T., "A Design Approach and Selected Wind-Tunnel Results at High Subsonic Speeds for Wing-Tip Mounted Winglets", NASA N D-8260, 1976
- [3] Whitcomb, R. T., "Methods for Reducing Aerodynamic Drag", NASA Conference Publication 2211, Proceedings of Dryden Symposium, California 1981
- [4] Maughmer, M. D., Timothy, S. S., and Willits, S. M., "The Design and Testing of a Winglet Airfoil for Low-Speed Aircraft", AIAA Paper 2001-2478, 2001

- [5] McLean, D., “Wingtip Devices: What They Do and How They Do It” presented at the Boeing Performance and Flight Operations Engineering Conference, 2005.
- [6] Lambert, D., “Numerical Investigation of Blended Winglet Effects on Wing Performances, report” Liege University; 2007.
- [7] [http://www.boeing.com/commercial/757family/pf/pf\\_facts.html](http://www.boeing.com/commercial/757family/pf/pf_facts.html).
- [8] <http://www.winggrid.ch/2014>
- [9] Smith, M. J., Komerath N., Ames, R., and Wong, O., “Performance Analysis OF A Wing with Multiple Winglets” American Institute of Aeronautics and Astronautics (AIAA-2407), 2001.
- [10] Versteeg, H., and Malalasekera, W. “An Introduction to Computational Fluid Dynamics: The Finite Volume Method” Longman, 1995.
- [11] FLUENT Documentation. © Fluent Inc. (2005).
- [12] Beehook, A. and Wang, J., “Aerodynamic Analysis of Variable Cant Angle Winglets for Improved Aircraft Performance”, Proceedings of the 19th International Conference on Automation & Computing, Brunel University, London, UK, 13-14 September, 2013.
- [13] Abdelghany, E.S. “Effect of Winglet Shape on Aircraft Wing Aerodynamic Performance”, PhD thesis, Mechanical Power Engineering, Cairo University, Egypt, 2015.
- [14] Versteeg, H., and Malalasekera, W. “An Introduction to Computational Fluid Dynamics: The Finite Volume Method” Longman, 1995.

**Nomenclature**

List of symbols			
b	Span length of wing	<b>Greek Letters</b>	
C	Chord length	$\alpha$	Angle of attack
$C_L$	Lift coefficient	$\varepsilon$	Turbulence dissipation rate
$C_D$	Drag coefficient	$\mu$	Dynamic viscosity
$\rho$	Density		
<b>List of Abbreviations</b>			
AOA	Angle of attack		
L	Length	AR	Aspect ratio of wing
M	Mach number	CFD	Computational Fluid Dynamics
S	Reference area		
P	Pressure value		
R	Radius		
Re	Reynolds number, $Re = \rho U C / \mu$		
t	Time		
T	Temperature		